

Evaluation of Recirculation Time in Bubble Train Flow by Using Direct Numerical Simulation

Hassanvand, Amin⁺*

*Department of Polymer Engineering, Faculty of Engineering, Lorestan University,
P.O. Box 68158144316 Khorramabad, I.R. IRAN*

Hashemabadi, Seyed Hassan

*Computational Fluid Dynamics Research Laboratory, School of Chemical Engineerin, Iran University of
Science and Technology, Tehran, I.R. IRAN*

ABSTRACT: *In this research, hydrodynamics of the Bubble Train Flows (BTF) in circular capillaries has been investigated by Direct Numerical Simulation (DNS). The Volume of Fluid Based (VOF) interface tracking method and streamwise direction periodic boundary conditions has been applied. The results show that there exists an appropriate agreement between DNS and experimental correlation results. The recirculation time as an important parameter, which affects the mass transfer of gas-liquid slug flow through the capillaries channel, has been calculated. The effects of different parameters such as capillary length, capillary diameter, unit cell length, and surface tension on recirculation time have been investigated. Afterwards, the DNS based correlation has been proposed for BTF recirculation time in a circular capillary.*

KEYWORDS: *Recirculation time; Bubble Train Flows (BTF); Direct Numerical Simulation (DNS); Volume Of Fluid (VOF); Circular Capillaries.*

INTRODUCTION

Monolith reactors are increasingly considered for multiphase catalytic reactions such as hydrogenations [1], hydrodesulphurization [2], oxidations [3], bioremediation [4] and Fischer–Tropsch synthesis [5]. These reactors have shown many advantages over conventional reactors such as high catalytic surface concentration, high mass transfer rate, low pressure drop, and ease of scale up. In monoliths, the predominant flow pattern is a Bubble-Train Flow (BTF) of elongated bubbles. BTF regime is an unsteady periodic flow of identical bubbles in regular sequence form. In this flow regime the bubbles, which

are separated by liquid slugs, fill almost the entire channel cross-section and travel with the same axial velocity. Optimization of mass transfer in monolith reactors requires profound understanding of the principle transport processes. The mass transfer from Taylor bubble to surrounding liquid slug takes place by two different modes. The first mode is the mass transfer to liquid film, flowing down the sides of the bubble, and the second one is the mass transfer from the two bubble capes to liquid slug. This mode of mass transfer is strongly influenced by radial mixing of the liquid moving as a slug [6].

* To whom correspondence should be addressed.

+ E-mail: amin.hassanvand@gmail.com

1021-9986/2016/2/93-104

12/\$/6.20

Radial mixing in bubble train flow in capillaries is affected by the length and frequency of bubbles. Some researchers reported that the length and frequency of bubbles plays a crucial role in heat and mass transfer enhancement in BTF regime. *Horvath et al.* calculated the radial mixing in slug flow through circular pipes by the bulk controlled reaction rates, measured in tubes with immobilized enzyme on the inner wall [7]. They reported that the radial mass transport in BTF regime increases rapidly with decreasing the liquid slug length. The experimental data reveals the remarkable effects of liquid slug and gas bubble hydrodynamics on mass transport in BTF regime.

The parameter that can be used as an index of radial mixing in BTF regime is recirculation time [8]. The estimation of recirculation time in BTF regime needs the detailed knowledge of its hydrodynamics. At this point, numerical simulations provide a beneficial tool to explore the hydrodynamics characteristics of the multiphase regime. Due to increase in computational power, multiphase Direct Numerical Simulation (DNS) become feasible. In this approach the flow field is obtained by solving the Navier-Stokes equation and appropriate interface capturing technique. There are different tracking methods for simulation of multiphase flow; some researchers used these methods to simulate Taylor bubble, such as VOF [9], Level set [10], and marker point [11]. Among these methods, Volume Of Fluid (VOF) is the most widely used method.

In literature, the hydrodynamics of BTF regime was simulated both in entire capillary length and in a single unit cell. Modeling of BTF regime in entire capillary length is very difficult and needs a high computational cost. Some researchers have modeled the BTF regime in entire capillary length [12-16]. Modeling of BTF regime by this method requires only the superficial velocities of two phases as an input and the void fraction, the bubble velocity are calculated as a part of the solution. However, when using such an approach, a long computational domain is required to obtain fully developed BTF regime [17]. Moreover, it needs a refined computational grid in order to capture flow features accurately.

Some researchers have modeled fully developed BTF regime in a single unit cell where liquid flows over the stationary bubble and the moving channel wall [18-22]. This approach not only can reduce the computational

complexity significantly, but also requires flow parameters such as the slug length, void fraction and the bubble velocity as input parameters. In this approach mixture velocity was specified at the inlet and fully developed boundary condition at the outlet. The wall velocity has been guessed initially and then iteratively updated until the bubble no longer moved in axial direction, so this method also needs a large computational effort.

Another approach to model BTF regime is combination of the above methods, in which one unit cell is considered and a bubble moves through this cell [23-26]. In this approach the periodic boundary conditions are used in the streamwise direction. The use of periodic boundary conditions requires a special treatment of the pressure term in momentum equations. To this aim, a reduced pressure is defined and the buoyancy force and the axial pressure gradient appear as source terms in the Navier-Stokes equation. With these source terms the bubble moves up and after elapsing enough run time the bubble shape eventually becomes steady. This approach has been used for simulating the hydrodynamics of BTF regime in a circular capillary in this study.

On the grounds of this fact that the mass transfer in BTF regime is strongly affected by the recirculation time in liquid slug, in this work DNS has been used for calculating the recirculation time. In this paper we investigate, to our knowledge for the first time, the effects of parameters such as capillary length, capillary diameter, unit cell length, and surface tension on recirculation time in laminar BTF through circular capillary. Based on the results of DNS a predictive correlation has been proposed for BTF recirculation time in a circular capillary.

MATHEMATICAL MODELING

Hydrodynamics

Fig. 1 shows the computational set-up for two dimensional axisymmetric simulation of laminar bubble train flow. The coordinate system is defined by taking y as axial direction and x as the radial direction. The gravity vector points in the negative y -direction. The boundary conditions used in this study have been shown in Fig. 1. In order to simulate bubble train flow, the approach of *Gidersa et al.* [23] has been used.

Two phase computations and interface tracking in this work are based on the VOF method. In the VOF model,

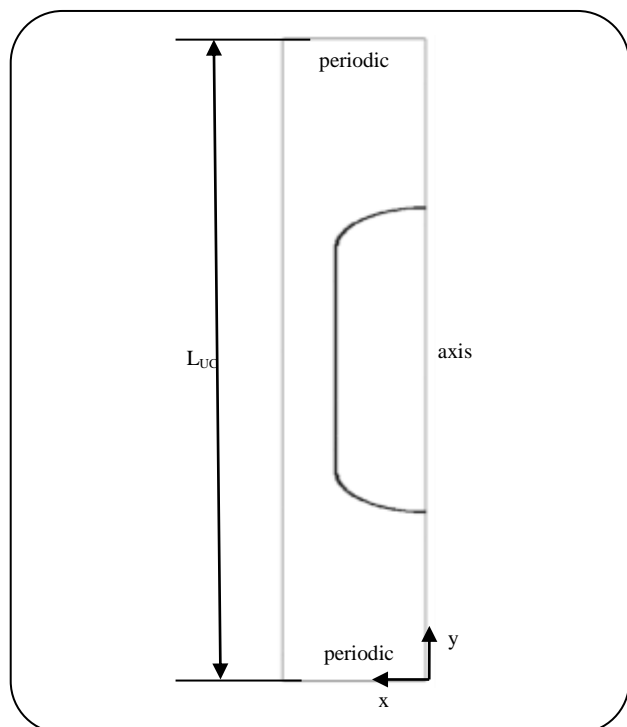


Fig. 1: Schematic of computational set-up for simulation of bubble train flow.

the variables such as pressure and velocity are shared by both phases and correspond to volume-averaged values. The volume-averaged conservation equations for mass and momentum describing the flow of two immiscible incompressible fluids are respectively:

$$\frac{\partial \rho_m}{\partial t} + \nabla \cdot (\rho_m \mathbf{u}_m) = 0 \quad (1)$$

$$\frac{\partial}{\partial t} (\rho_m \mathbf{u}_m) + \nabla \cdot (\rho_m \mathbf{u}_m \mathbf{u}_m) =$$

$$-\nabla p + \nabla \cdot \mu_m (\nabla \mathbf{u}_m + (\nabla \mathbf{u}_m)^T) + \rho_m \mathbf{g} + \mathbf{f}_\sigma$$

Mixture density and dynamic viscosity are determined by volume fraction averaging.

$$\rho_m = \alpha \rho_g + (1 - \alpha) \rho_L \quad (3)$$

$$\mu_m = \alpha \mu_g + (1 - \alpha) \mu_L$$

Gas liquid surface tension creates a pressure jump across the interface and in equilibrium its gradient must be equal to extra body force inserted in the momentum equation. The momentum equation is written for the whole domain but this force is noticeable only at interface

by giving the transitional area a finite thickness. The discontinuous pressure jump can be calculated [27]:

$$\mathbf{f}_\sigma = -\sigma \left(\nabla \cdot \left(\frac{\nabla \alpha}{|\nabla \alpha|} \right) \right) (\nabla \alpha) \quad (4)$$

It is thus necessary to know the gas volume fraction in the entire computational domain. Tracking the interface between phases is accomplished by the solution of a continuity equation for the volume fraction as follows:

$$\frac{\partial \alpha}{\partial t} + \mathbf{u} \cdot \nabla \alpha = 0 \quad (5)$$

When computational cell is completely filled with gas phase, α is equal one and in reverse is zero. The interface can be found in the cells with $0 < \alpha < 1$.

Because the pressure p in equation (2) is not periodic, thus equation must be recast in a form which is suitable for a domain with periodic boundary conditions. For this purpose the pressure is split as follows:

$$\rho \equiv P - \rho_L \mathbf{g} \hat{\mathbf{e}}_y \cdot \mathbf{x} + \quad (6)$$

$$\left(\frac{\rho|_{y=L_{UC}} - \rho|_{y=0} + \rho_L \mathbf{g} L_{UC}}{L_{UC}} \right) \hat{\mathbf{e}}_y \cdot \mathbf{x} =$$

$$P + \rho_L \mathbf{g} \cdot \mathbf{x} + \frac{\Delta \rho}{L_{UC}} \hat{\mathbf{e}}_y \cdot \mathbf{x}$$

By this modification on pressure then the momentum equation can be written as

$$\frac{\partial}{\partial t} (\rho_m \mathbf{u}_m) + \nabla \cdot (\rho_m \mathbf{u}_m \mathbf{u}_m) = \quad (7)$$

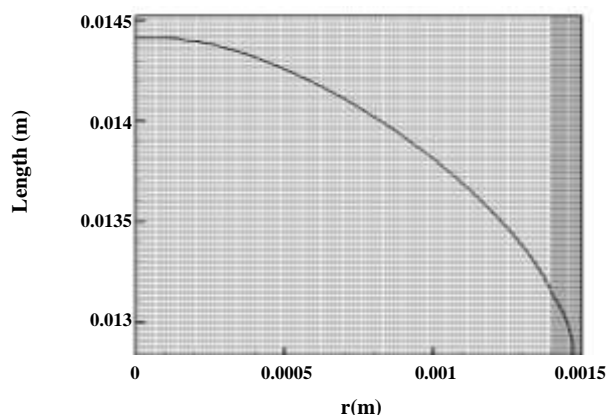
$$-\nabla P + \nabla \cdot \mu_m (\nabla \mathbf{u}_m + (\nabla \mathbf{u}_m)^T) + (\rho_m - \rho_L) \mathbf{g} - \frac{\Delta \rho}{L_{UC}} + \mathbf{f}_\sigma$$

Discretization and solution method

The Fluent 6.3.26 is used to model two-dimensional, axisymmetric, transient, two-phase Taylor flow in a circular capillary. The volume-of-fluid method is used to identify the gas-liquid interface by solving a volume fraction equation for one of the phases. An explicit geometric reconstruction scheme is used to represent the interface by using a piecewise-linear approach [28]. The fluids are assumed to be incompressible and isothermal and to have constant fluid properties. The finite volume method [29] was used to discretize the transport equations.

Table 1: Comparison of the calculated liquid film thickness and experimental correlation ($\alpha=0.324$).

Near wall mesh size (μm)	Computational Time (hr)	Liquid film thickness (μm) DNS	Liquid film thickness (μm) correlation [31]
7.5	55	46	36
3.75	140	40	36
1.875	486	38	36

**Fig. 2: Typical computational grid for DNS simulation ($L_{uc}=15\text{mm}$, $d_c=3\text{mm}$, $\varepsilon_G=0.324$, and $\sigma=0.072\text{ N/m}$).**

Convection terms in momentum equations were discretised with a High Resolution (HR) differencing scheme proposed by *Jasak* [30]. Diffusive flux terms in momentum equation were divided to orthogonal and non-orthogonal terms. The non-orthogonal terms could be calculated by previous time step values and corrected in an internal loop. Due to computational expense of this method and because the non-orthogonality of meshes was minor and time step size was also small with respect to other time scales in this flow process, no correction was executed in solution algorithm. Volume fraction needs to be smoothed in order to calculate the curvature and consequently f_{σ} , *Brackbill* [27] used a B-spline as an interpolation function to smooth the volume fraction and this method was used in the present work.

RESULTS AND DISCUSSION

Grid-Independence Study

In order to take account of the hydrodynamics of BTF regime, uniform structured grid was used. Fig. 2 shows one of the computational grid (the interval size/capillary diameter is 1/400 near the wall and for flow domain is 1/200), used in this study. One of the most important parameters in the BTF regime is the thickness of liquid

film around the Taylor bubble, in this work this thickness is chosen as a parameter that distinguishes the grid size. Owing to this reason, the grid size has been refined in the vicinity of the wall (Fig. 2). Table 1 compares the numerical calculated film thickness with the one that obtained using Aussillous and Quere empirical correlation [31]. In this table the results for 3mm capillary with unit cell length of 15 mm and gas volume fraction of 0.324 for the air ($\rho_G=1.2\text{ kg/m}^3$, $\mu_G=1.78\text{e-}05\text{ Pa s}$) and water ($\rho_L=1000\text{ kg/m}^3$, $\mu_L=0.001\text{ Pa s}$) system has been reported. A total run time of 1 s was used for each run of the simulations. The 7.5, 3.75 and 1.875 μm near wall grid on a cluster workstation (4 Intel® Xeon® E5335 Quad Core, 2 GHz 8 MB cash CPU with 16 GB RAM) took 55, 140 and 486 h for a simulation run. In these cases, by grid refinement the time step also becomes smaller to fix the Courant number at constant value. As shown in this table, the gaining result deviation for near wall grid size of 3.75 μm and 1.875 μm is less than 5%. From the grid independency analysis, the grid size of 3.75 μm is chosen for near wall and the grid size of 7.5 μm was used for the reset of domain. With this grid size the time step of $4\times 10^{-6}\text{ s}$ leads to appropriate results.

Solution Initialization

In Direct Numerical Simulation method explained in the modeling section, the gas volume fraction in unit cell must be set at the beginning of the simulation. Due to low Mach number (<0.3) gas is assumed incompressible, this volume fraction remains constant during the simulation and the two phase flow hydrodynamics is affected by this value. At high gas volume fraction the initial shape of gas bubble may leads to wrong results. Fig. 3 shows the effect of the initial gas volume fraction on air-water two phase hydrodynamics in 2mm capillary with 8mm unit cell length and 0.76 gas volume fraction. As can be seen in Fig. 3A and Fig. 3B, when the solution is initialized with the rectangular bubble shape, after a while the front and the rear of the bubble join together and the Taylor

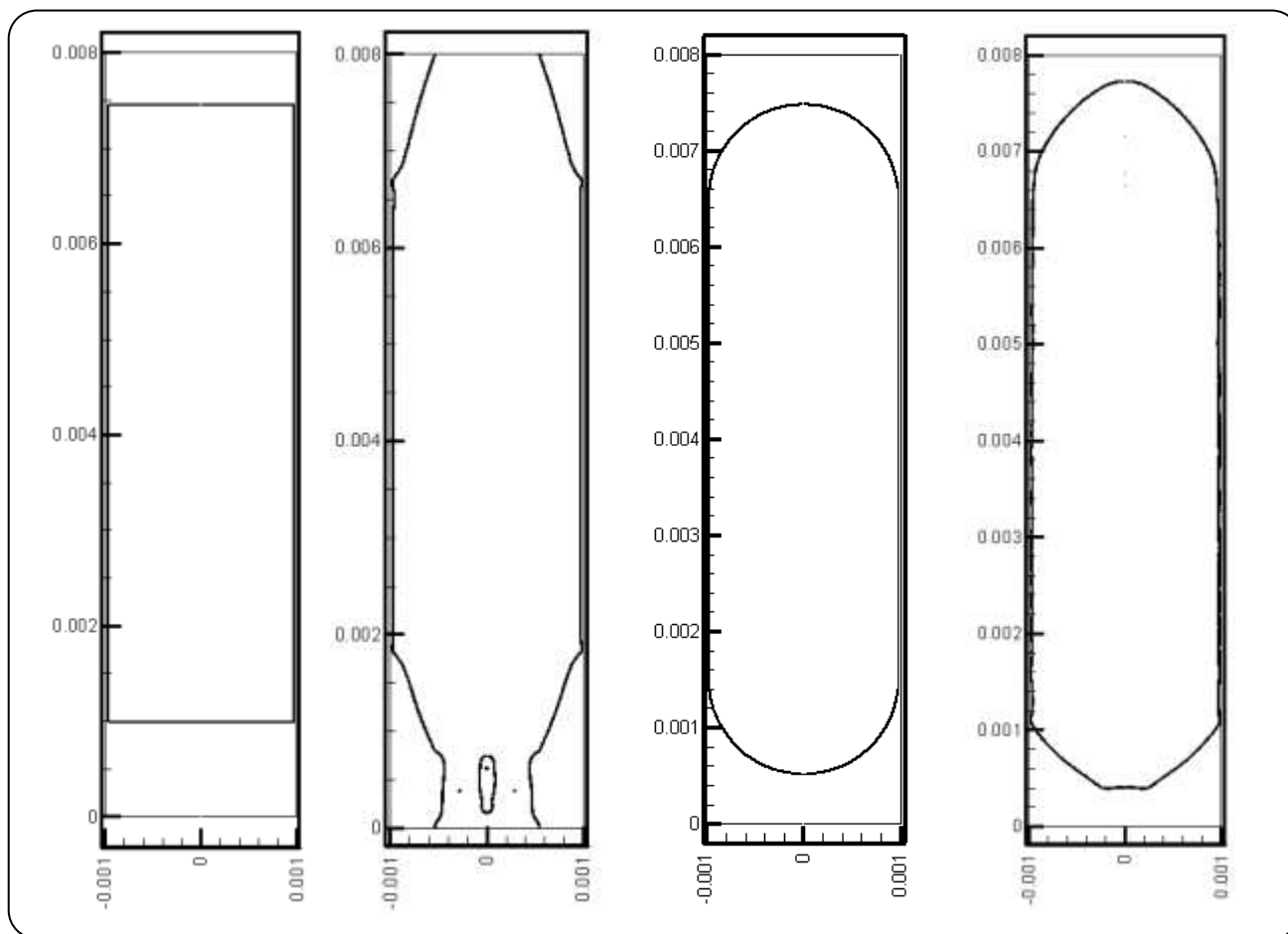


Fig. 3: The effect of the initial Taylor bubble shape on two phase hydrodynamics ($L_{UC}=8\text{mm}$, $d_c=2\text{mm}$, $\epsilon_g=0.76$, and $\sigma=0.072\text{ N/m}$).

bubble is broken. Fig. 3C and Fig. 3D show that for the mentioned condition when the initial bubble shape consists of rectangle and two caps, the desired flow regime is obtained and after enough simulation time the steady bubble shape is formed (Fig. 3D). Our numerical simulations show that for lower gas volume fraction (less than 0.5) any initial bubble leads to the good results, but for higher gas volume fraction the initial bubble diameter must be slightly lower than the pipe diameter in order to obtain acceptable results.

Fig. 4 shows the mechanisms of air bubble formation and rising in 3mm capillary with 15mm unit cell length and 0.17 gas volume fraction. The initial bubble shape consists of rectangle and two capes. As can be seen in this Fig., at the starting of the simulation the liquid film around the bubble is reduced by decreasing the bubble length. This process continues until the liquid film reaches its equilibrium condition and no longer changes, and the bubble starts rising

through the capillary, if at this stage we do not have mass transfer, there is no variation in bubble shape.

Validation

The results for air-water BTF hydrodynamics simulation has been verified by drawing a comparison between the length of liquid slug from simulations and the experimental based correlations (Kreutzer[32] and Liu *et al.*[33]). The liquid slug length has been obtained by the axial distance between the front and back of the bubble. Comparison between the results of simulation and empirical correlations are depicted in Table 2. As it can be seen in this Table, there is an acceptable agreement between the simulation and correlation results. The results illustrate that the numerical value of slug length has a maximum error of 26.87% and 43.07% compared to the Kreutzer (Equation (8)) and Liu *et al.* (Equation (9)) correlations, respectively.

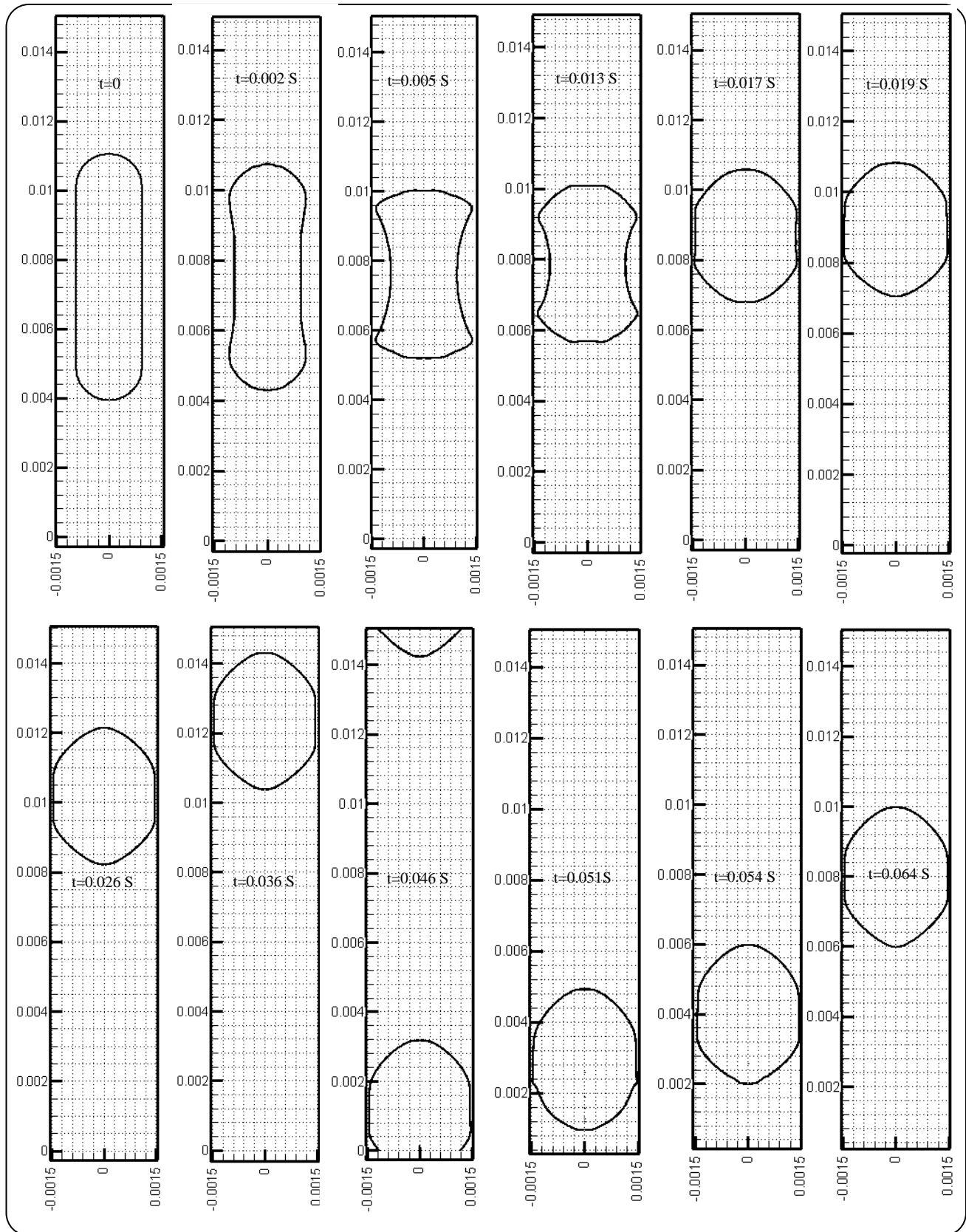


Fig. 4: Up: bubble formation mechanism, down: bubble rising ($L_{bc}=15\text{mm}$, $d_c=3\text{mm}$, $\varepsilon_g=0.17$ and $\sigma=0.072$ N/m).

Table 2: The comparison between the simulation and the correlations results.

σ (N/m)	ε_G	L_S (DNS)(mm)	L_S (mm) [32]	Error (%)	L_S (mm) [33]	Error (%)
0.072	0.170	11.20	11.43	-2.00	14.28	-21.55
0.072	0.324	8.73	6.71	30.09	11.94	-26.87
0.072	0.591	5.22	6.02	-13.42	6.78	-23.09
0.0215	0.324	7.26	5.64	28.79	9.13	-20.46
0.030	0.324	8.51	5.95	43.07	9.79	-13.08
0.040	0.324	8.47	5.98	41.67	10.09	-16.01
0.050	0.324	8.34	6.05	37.81	10.37	-19.55

$$\frac{L_S}{d_c} = \frac{\varepsilon_L}{-0.00141 - 1.556\varepsilon_L^2 \ln(\varepsilon_L)}, \quad \varepsilon_L \approx \frac{U_{LS}}{U_{LS} + U_{CS}} \quad (8)$$

$$\frac{U_{TP}}{\sqrt{L_S}} = 0.088 \text{Re}_G^{0.72} \text{Re}_L^{0.19} \quad (9)$$

$$\text{Re}_G = \frac{\rho_C U_{CS}}{\mu_C}, \quad \text{Re}_L = \frac{\rho_L U_{LS}}{\mu_L}$$

The results depict that the agreement is better with Kreutzer correlation. This might be attributed to this fact that the volume fraction and the ratio of gas/liquid velocities are included in Kreutzer correlation. The higher discrepancy of the DNS results with Liu et al. correlation has been also stated by *Shao et al.* [34]. It could be related to the use of gas and liquid velocities separately rather than their ratio in this correlation. *Shao et al.* [34] stated that the bubble length is affected by the gas/liquid flow rate or velocity ratio more than the other parameters. In each DNS case the bubble velocity, superficial liquid and gas velocities are calculated as follow:

$$U_B = \frac{\sum \alpha u}{\sum \alpha}, \quad U_{LS} = \varepsilon_G U_B \quad (10)$$

$$U_{GS} = U_{\text{avg}} - \varepsilon_G U_B$$

Based on the above values the liquid slug length is calculated from Equations. (8) and (9).

These comparisons lend confidence to the Direct Numerical Simulation results that have been reported in the next section. In this study air ($\rho_G=1.2 \text{ kg/m}^3$, $\mu_G= 1.78\text{e-}05 \text{ Pa s}$) and water ($\rho_L=1000 \text{ kg/m}^3$, $\mu_L= 0.001 \text{ Pa s}$) were considered for gas and liquid phase, respectively.

Effect of Gas Volume Fraction

The simulation results for five cases are considered for studying the effect of gas volume fraction on recirculation time. In these cases the capillary diameter and surface tension are 3mm and 0.072 N/m respectively. Five different gas volume fractions (0.17, 0.33, 0.5, 0.6, and 0.76) are used for performing the simulations. In order to calculate the recirculation time the definition of *Thulasidas et al.* [35] has been used. They defined the non-dimensional time which quantified the intensity of recirculation in liquid slug as follow

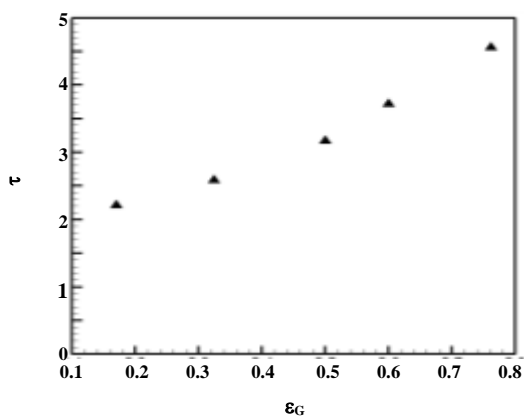
$$\tau \equiv \frac{T_L}{T_s} = \frac{T_L U_B}{L_s} \quad (11)$$

The non-dimensional recirculation time is the ratio of the time needed for the liquid to move from one end of the slug to the other end (T_L) over the time needed by the liquid slug to travel a distance of its own length (T_s). By decreasing the recirculation time, the faster mixing take place in liquid slug and the mass transfer from bubble caps can be promoted.

Fig. 5 depicts the gas volume fraction effect on recirculation time, as can be seen in this Fig. the recirculation time increases with growing gas volume fraction. The increase in recirculation time can be explained by investigating the variation of parameters that influenced this quantity by increasing gas volume fraction. According to recirculation time definition (Equation (8)), three parameters (U_B , L_s , and T_L) affect this quantity. Table 3 depicts the effect of gas volume fraction on U_B , L_s , and T_L . The results show that by enhancing the gas volume fraction, L_s and T_L reduce and in other hand the U_B increases. With the bubble velocity (U_B) promotion and the liquid slug length (L_s) reduction,

Table 3: The effect of gas volume fraction (ε_G) on the parameters that affect the recirculation time.

ε_G	U_B (m/s)	L_s (mm)	T_L (s)	Ca	τ
0.17	0.198	11.10	0.124	0.00275	2.21
0.33	0.369	8.73	0.061	0.00512	2.59
0.5	0.726	5.82	0.025	0.01008	3.16
0.6	0.920	4.47	0.018	0.01277	3.71
0.76	1.137	1.43	0.006	0.01579	4.56

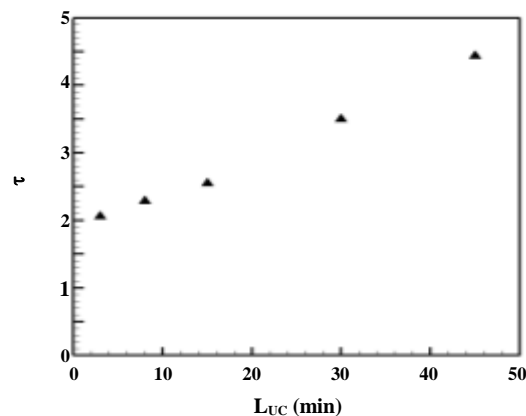
**Fig. 5: The effect of gas volume fraction (ε_G) on recirculation time ($L_{UC}=15$ mm, $d_c=3$ mm, and $\sigma=0.072$ N/m).**

the recirculation time increases, whereas reducing of T_L decreases the recirculation time.

Table 3 depicts that the effects of U_B and L_s on recirculation time are more severe than the effect of T_L , therefore the recirculation time increases with enhancement of gas volume fraction. In higher gas volume fraction, this mixing index of two phase flow through the capillary channel grows up more considerably. Consequently the results show that increasing the gas volume fraction with constant unit cell length increases the recirculation time and reduces the mass transfer between Taylor bubble and liquid slug. Table 3 also illustrates that increasing the capillary number increases the recirculation time. *Thulasidas et al.* experimentally show that the recirculation time increases by promotion of the capillary number [35].

Effect of Unit Cell Length

In order to study the unit cell length effects on the recirculation time, the simulation results for five different cases are considered. In these cases the capillary diameter, gas volume fraction, and surface tension are 3mm,

**Fig. 6: The effect of L_{UC} on recirculation time ($d_c=3$ mm, $\sigma=0.072$ N/m, and $\varepsilon_G=0.324$).**

0.324, and 0.072 N/m respectively and five different unit cell lengths (3, 8, 15, 30, 45 mm) are used for performing the simulations. Fig. 6 shows the unit cell length effect on recirculation time, as can be seen from this Fig. by increasing the unit cell length the recirculation time increases. DNS results show increase in L_s , T_L , and U_B by promotion of the unit cell length at constant gas volume fraction but the effects of U_B and T_L on recirculation time are more considerable than the effect of L_s , therefore the recirculation time increases with increasing unit cell length. The simulations reveal that decreasing the unit cell length decreases the recirculation time and enhances the mass transfer from Taylor bubble.

Effect of Capillary Diameter

Fig. 7 shows the effect of capillary diameter on recirculation time. In these cases the capillary length, gas volume fraction and surface tension are respectively 15mm, 0.76, and 0.072 N/m. Six different capillary diameters (0.5, 1, 1.5, 2, 2.5, and 3 mm) are simulated. The results illustrate that by increasing the capillary diameter the recirculation time enhances. However from

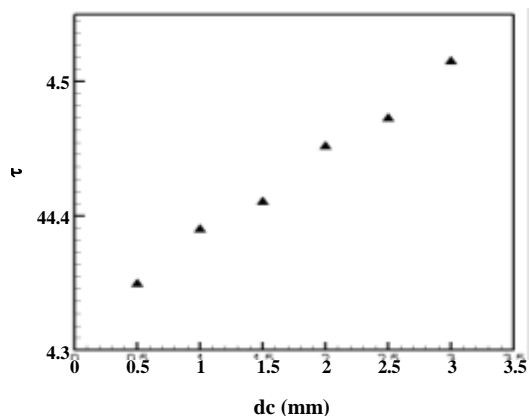


Fig. 7: The effect of capillary diameter on recirculation time ($L_{UC}=15\text{mm}$, $\sigma=0.072\text{ N/m}$, and $\varepsilon_G=0.76$).

this Fig. show that with six times the capillary diameter the difference between the maximum and minimum recirculation time is less than 5%. These results illustrate that the effect of capillary diameter on recirculation time is minor and this effect can be neglected.

Effect of Surface Tension

The influence of surface tension on recirculation time is shown in Fig. 8. In order to simulate the effect of surface tension on recirculation time six different surface tension are taking to account. In these set of simulations the capillary length, capillary diameter and gas volume fraction are 15mm, 3mm, and 0.324 respectively. Six different surface tensions (0.0215, 0.03, 0.04, 0.05, 0.06, and 0.072 N/m) are considered in the simulations. The results show with increasing the surface tension the recirculation time reduces. Fig. 9 shows the produced Taylor bubble in capillary for different values of surface tension. As can be seen in this Fig., the liquid film thickness around the bubble and the Taylor bubble length has been increased by decreasing the surface tension.

DNS based Correlation for Recirculation Time

The following correlation, based on the DNS results, has been proposed for calculation of the recirculation time in circular capillary.

$$\tau = \frac{1}{1 - 1.68C_a^{0.187}} \quad (12)$$

Fig. 10 compares the recirculation time predicted from DNS and the proposed correlation for Capillary

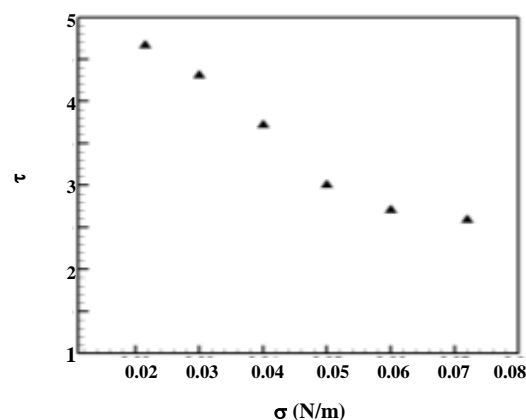


Fig. 8: The effect of surface tension on recirculation time ($L_{UC}=15\text{mm}$, $d_c=3\text{mm}$, and $\varepsilon_G=0.324$).

number from 0.0018 to 0.018. As can be seen in Fig. 10, the correlation accuracy is acceptable in this range of Capillary number. In this correlation Capillary number embraces the effects of different parameters on recirculation time. DNS results show that by enhancing the unit cell length and the gas volume fraction the bubble velocity increases, which causes the Capillary number and recirculation time to grow up, respectively.

CONCLUSIONS

In this study Direct Numerical Simulation (DNS) has been used for simulating the hydrodynamics of the Bubble Train Flows (BTF) regime in circular capillaries. The accuracy of DNS model has been proved by comparing the DNS and correlation results. The recirculation time, as an important parameter which influenced the mass transfer from the BTF regime, in liquid slug has been calculated. Furthermore, the effects of different parameters such as capillary length, capillary diameter, unit cell length and surface tension on recirculation time have been investigated. The results show that increasing the unit cell length and the gas volume fraction increase the recirculation time; however, increasing the surface tension decreases the recirculation time. This work reveals that at constant physical properties the efficient mass transfer in BTF regime is obtained by small unit cell length and low gas volume fraction. Finally, the DNS based correlation has been proposed for recirculation time calculation in bubble train flow inside a circular capillary.

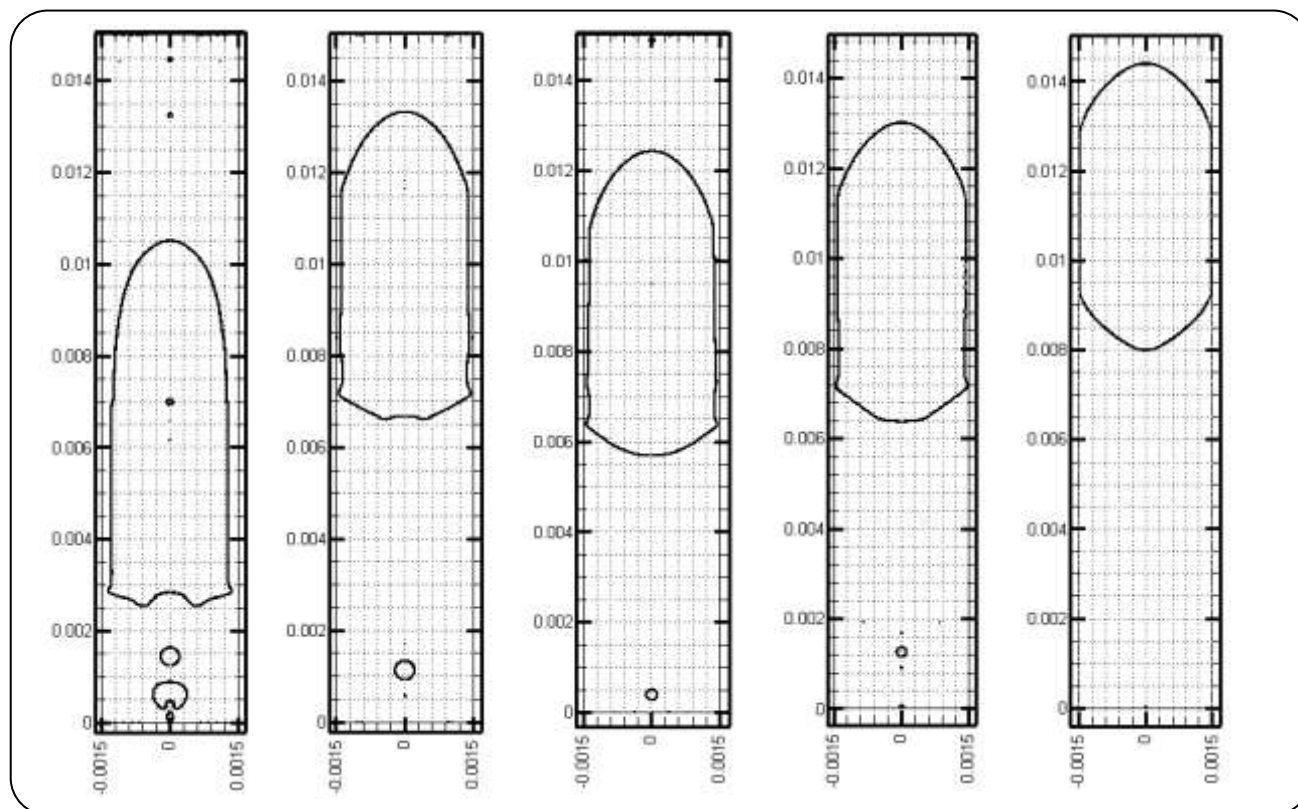


Fig. 9: Effect of surface tension on bubble shape ($L_{UC}=15\text{mm}$, $d_c=3\text{mm}$, and $\varepsilon_G=0.324$).

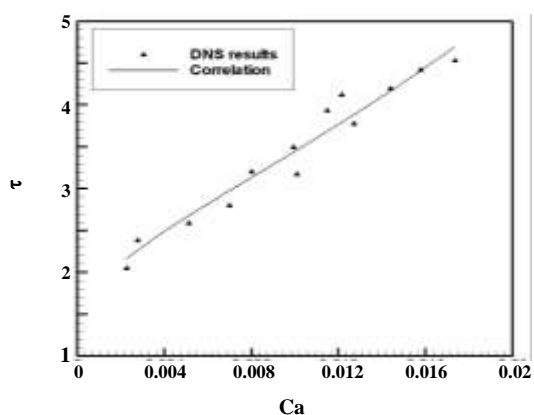


Fig. 10: Comparison between DNS and the proposed correlation for $0.0018 < Ca < 0.018$.

Nomenclature

Ca	Capillary number $\mu_L U_B / \sigma$, dimensionless
d_c	Capillary diameter, m
\hat{e}_y	Unit vector in y-direction
f_σ	Surface tension force, N
g	Gravity acceleration, m/s^2
\mathbf{g}	Gravity vector, m/s^2
L_s	Liquid slug length, m

L_{UC}	Unit cell length, m
p	Pressure, Pa
P	Periodic part of pressure, Pa
$\Delta \hat{p}$	Non-hydrostatic pressure drop across L_{UC} , Pa
Re	Reynolds number, dimensionless
u	Velocity, m/s
U_{avg}	Average velocity at capillary cross section, m/s
U_B	Bubble velocity, m/s
U_{GS}	Superficial gas velocity, m/s
U_{LS}	Superficial liquid velocity, m/s
U_{TP}	Two-phase superficial velocity ($U_{GS} + U_{LS}$), m/s
\mathbf{x}	Position vector, m

Greeks

α	Local gas volume fraction, dimensionless
ε_G	Overall gas volume fraction in domain, dimensionless
ε_L	Velocities ratio in Kreutzer correlation, dimensionless
μ	Dynamic viscosity, Pas
ρ	Density, kg/m^3
σ	Surface tension, N/m

Subscripts

B	Bubble
G	Gas
L	Liquid
m	Mixture quantity

Received : Jun. 25, 2014 ; Accepted : Jan. 4, 2016

REFERENCES

- [1] Nijhuis T.A., Dautzenberg F.M., Moulijn J.A., Modeling of Monolithic and Trickle-Bed Reactors for the Hydrogenation of Styrene, *Chem. Eng. Sci.*, **58**: 1113-1124 (2003).
- [2] Irandoust S., Gahne O., Competitive Hydrodesulfurization and Hydrogenation in a Monolithic Reactor, *AIChE J.*, **36**: 746-752 (1990).
- [3] Klinghoffer A.A., Cerro R.L., Abraham M.A., Influence of Flow Properties on the Performance of the Monolith Froth Reactor for Catalytic Wet Oxidation of Acetic Acid, *Ind. Eng. Chem. Res.*, **37**: 1203-1210 (1998).
- [4] Quan X.C., Shi H.C., Zhang Y.M., Wang J.L., Qian Y., Biodegradation of 2,4-Dichlorophenol in an Air-Lift Honeycomb-Like Ceramic Reactor, *Process Biochem.*, **38**: 1545-1551 (2003).
- [5] Khassin A.A., Yurieva T.M., Sipatrov A.G., Kirillov V.A., Chermashmentseva G.K., Parmon V.N., Fischer-Tropsch Synthesis Using a Porous Catalyst Packing: Experimental Evidence of an Efficient Use of Permeable Composite Monoliths as a Novel Type of Fischer-Tropsch Synthesis Catalyst, *Catal. Today*, **79-80**: 465-470 (2003).
- [6] van Baten J. M., Krishna R., CFD Simulations of Mass Transfer from Taylor Bubbles Rising in Circular Capillaries, *Chem. Eng. Sci.*, **59**: 2535-2545 (2004).
- [7] Horvath C., Solomon B.A., Engasser J.M., Measurement of Radial Transport in Slug Flow Using Enzyme Tubes, *Ind. Eng. Chem. Res.*, **12**: 1203-1210 (1973).
- [8] Kececi S., Wörner M., Soyhan H. S., Recirculation Time and Liquid Slug Mass Transfer in co-Current Upward and Downward Taylor Flow, *Catal. Today*, **147S**: 125-131 (2009).
- [9] Akbar M.K., Ghiaasiaan S.M., Simulation of Taylor Flow in Capillaries Based on Volume-of-Fluid Techniques, *Ind. Eng. Chem. Res.*, **45**: 5396-5403 (2006).
- [10] Fukagata K., Kasagi N., Ua-arayaporn P., Himeno T., Numerical Simulation of Gas-Liquid Two-Phase Flow and Convective Heat Transfer in a Micro Tube, *Int. J. Heat Fluid Flow*, **28**: 72-82 (2007).
- [11] Muradoglu M., Stone H. A., Motion of Large Bubbles in Curved Channels, *J. Fluid Mech.*, **570**: 455-466 (2007).
- [12] Yang Z.L., Palm B., Sehgal B.R., Numerical Simulation of Bubbly Two-Phase Flow in a Narrow Channel, *Int. J. Heat Mass Trans.*, **45**: 631-639 (2002).
- [13] Qian D., Lawal A., Numerical Study on Gas and Liquid Slugs for Taylor Flow in a T-junction Microchannel, *Chem. Eng. Sci.*, **61**: 7609-7625 (2006).
- [14] Gupta R., Fletcher D. F., Haynes B. S., On the CFD Modelling of Taylor Flow in Microchannels, *Chem. Eng. Sci.*, **64**: 2941-2950 (2009).
- [15] Chen Y., Kulenovic R., Mertz R., Numerical Study on the Formation of Taylor Bubbles in Capillary Tubes, *Int. J. Therm. Sci.*, **48**: 234-242 (2009).
- [16] Shao N., Gavriilidis A., Angeli P., Flow Regimes for Adiabatic Gas-Liquid Flow in Microchannels, *Chem. Eng. Sci.*, **64**: 2749-2761 (2009).
- [17] Gupta R., Fletcher D.F., Haynes B.S., CFD Modeling of Heat Transfer in the Taylor Flow Regime, *Chem. Eng. Sci.*, **65**: 2094-2107 (2010).
- [18] Hassanvand A., Hashemabadi S. H., Direct Numerical Simulation of Mass Transfer from Taylor Bubble Flow Through a Circular Capillary, *Int. J. Heat and Mass Transfer*, **55**: 5959-5971 (2012).
- [19] Taha T., Cui Z. F., CFD Modelling of Slug Flow Inside Square Capillaries, *Chem. Eng. Sci.*, **61**: 665-675 (2006).
- [20] Wang S., Liu D., Hydrodynamics of Taylor Flow in Noncircular Capillaries, *Chem. Eng. Process.*, **47**: 2098-2105 (2008).
- [21] Feng J.Q., A Long Gas Bubble Moving in a Tube with Flowing Liquid, *Int. J. Multiphas Flow*, **35**: 738-746 (2009).
- [22] Kreutzer M.T., Kapteijn F., Moulijn J.A., Kleijn C.R., Heiszwolf J.J., Inertial and Interfacial Effects on Pressure Drop of Taylor Flow in Capillaries, *AIChE J.*, **51**: 2428-2440 (2005).
- [23] Ghidersa B.E., Wörner M., Cacuci D.G., Exploring the Flow of Immiscible Fluids in a Square Mini-Channel by Direct Numerical Simulation, *Chem. Eng. J.*, **101**: 285-294 (2004).

- [24] Wörner M., Ghidersa B., Onea A., [A Model for Residence Time Distribution of Bubble-Train Flow in Square Mini Channel Based on Direct Numerical Simulations Results](#), *Int. J. Heat Fluid Flow*, **28**: 83-94 (2007).
- [25] Özkan F., Wörner M., Wenka A., Soyhan H.S., [Critical Evaluation of CFD Codes for Interfacial Simulation of Bubble Train Flow in Narrow Channel](#), *Int. J. Numer. Meth. Fluids*, **55**: 537-564 (2007).
- [26] Keskin Ö., Wörner M., Soyhan H.S., Bauer T., Deutschmann O., Lange R., [Viscous Co-Current Downward Taylor Flow in a Square Mini-Channel](#), *AIChE J.*, **56**: 1693-1702 (2009).
- [27] Brackbill J.U., Kothe D.B., Zemach C., [A Continuum Method for Modeling Surface Tension](#), *J. Comput. Phys.*, **100**: 335-354 (1992).
- [28] Youngs D.L., [Time-Dependent Multi-Material Flow with Large Fluid Distortion](#), In: Morton K.W., Baines M.J. (Eds), "Numerical Methods for Fluid Dynamics", Academic Press, New York (1982).
- [29] Patankar S.V., "Numerical Heat Transfer and Fluid Flow", Taylor and Francis, Philadelphia (1980).
- [30] Jasak H., Weller H.C., Issa R.I., Gosman A.D., [High Resolution NVD Differencing Scheme for Arbitrarily Unstructured Meshes](#), *Int. J. Numer. Meth. Fluids*, **31**: 431-449 (1999).
- [31] Aussillous P., Quere D., [Quick Deposition of a Fluid on the Wall of a Tube](#), *Phys. Fluids*, **12**: 2367-2371 (2000).
- [32] Kreutzer M., "Hydrodynamics of Taylor Flow in Capillaries and Monolith Reactors", Delft University Press, Delft (2003).
- [33] Liu H., Vandu C.O., Krishna R., [Hydrodynamics of Taylor Flow in Vertical Capillaries: Flow Regimes, Bubble Rise Velocity, Liquid Slug Length, and Pressure Drop](#), *Ind. Eng. Chem. Res.*, **44**: 4884-4897 (2005).
- [34] Shao N., Salman W., Gavriilidis A., Angeli P., [CFD Simulations of the Effect of Inlet Conditions on Taylor Flow Formation](#), *Int. J. Heat Fluid Flow*, **29**: 1603-1611 (2008).
- [35] Thulasidas T.C., Abraham M.A., Cerro R.L., [Flow Patterns in Liquid Slugs During Bubble-Train Flow Inside Capillaries](#), *Chem. Eng. Sci.*, **52**: 2947-2962 (1997).